Int. J. Multiphase Flow Vol. 16, No. 1, pp. 123–138, 1990
Printed in Great Britain.

0301-9322/90 $3.00 + 0.00

CHF PREDICTION FOR HORIZONTAL TUBES

Y. L. WONG,[1] D. C. GROENEVELD[2] and S. C. CHENG[1]

[1]Department of Mechanical Engineering, University of Ottawa, Ottawa, Ontario K1N 6N5, Canada

[2]Thermalhydraulics Development Branch, Chalk River Nuclear Laboratories (CRNL), Atomic Energy of Canada Limited (AECL), Chalk River, Ontario K0J 1J0, Canada

(*Received* 29 *August* 1988; *in revised form* 29 *May* 1989)

Abstract—The mechanisms governing flow stratification in a horizontal tube have been investigated. Simplified models for the prediction of CHF in horizontal forced-convective flow were developed based on CHF in vertical flow using correction factors. The proposed models are compared with experimental data and show reasonable agreement.

Key Words: CHF, horizontal flow, stratified flow, correction factor

1. INTRODUCTION

Accurate prediction of the heat flux associated with the boiling crisis or critical heat flux (CHF) is important in nuclear reactor design and safety analysis, and in the design of industrial boilers and heat exchangers involving two-phase flow. It is also of importance in devices operating under subcooled or non-boiling conditions. Boiling may occur under off-design conditions or accident conditions and thus CHF may occur.

Over the years, hundreds of *ad hoc* correlations have been developed for the prediction of CHF in vertical flow. Most of them are applicable for a limited range of flow conditions only. Assessment of various published correlations was undertaken by ESDU (1986). They have recommended the CHF table look-up method published by Groeneveld *et al.* (1986b) for the prediction of CHF in vertical flow. However, prediction methods for CHF in horizontal flow are scarce and inaccurate; they are generally valid for a limited range of flow parameters only. One of the reasons for the poor performance of horizontal CHF correlations is the scarcity of horizontal CHF data.

The objective of this study is to develop a generalized CHF prediction method for horizontal flow. To determine the CHF for horizontal flow, Groeneveld *et al.* (1986a) suggested that the CHF for vertical flow be multiplied by a correction factor K_{hor}:

$$\mathrm{CHF}_{hor} = K_{hor} \times \mathrm{CHF}_{ver}. \quad [1]$$

This study is an attempt to derive an expression for the correction factor K_{hor} which is a function of mass flux, vapour quality, pressure and tube diameter.

2. CHF MECHANISMS

2.1. CHF Mechanisms for Vertical Flow

2.1.1. Subcooled and low-quality regions

The most commonly postulated mechanisms for CHF in subcooled and low-quality regions are (Hewitt 1982):

1. Near-wall bubble crowding and vapour blanketing.
2. Local overheating following microlayer evaporation from a nucleation site.
3. Burnout associated with vapour clot or slug formation.

Figure 1(a) illustrates schematically the near-wall bubble crowding and vapour blanketing mechanism. A "bubble boundary layer" builds up on the heated surface and is ultimately thick enough to prevent liquid migration to the surface, thus causing high liquid-superheat near the wall, resulting in departure from nucleate boiling (DNB) occurrence. The concept of boundary-layer

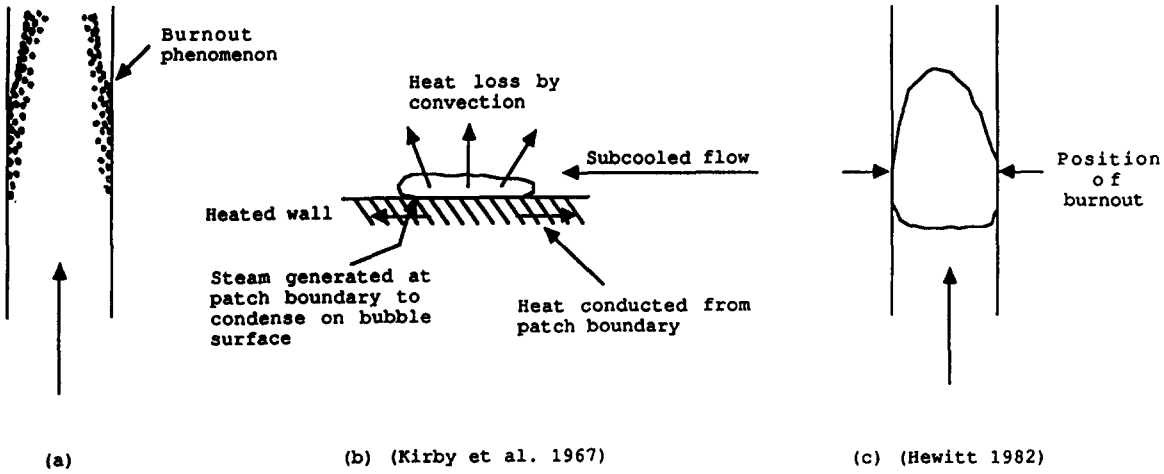

Figure 1. CHF mechanisms for low quality and subcooled boiling: (a) near-wall bubble crowding; (b) local overheating following bubble growth from a nucleation centre; (c) burnout associated with vapour clot or slug formation.

separation for the burnout phenomenon was proposed by Kutateladze & Leontiev (1966). Tong (1972) modified the boundary-layer separation theory by pointing out that the friction factor for a channel with a bubble boundary layer is much higher than that for a smooth tube because the liquid has to flow over a rougher surface, represented by the bubble boundary layer. He was able to derive a reasonably accurate semi-empirical correlation.

The second type of mechanism is shown schematically in figure 1(b). When a bubble grows at a nucleation site, "microlayer evaporation" occurs under the growing bubble, resulting in a disk of dry surface. The wall temperature at this dry patch rises rapidly and the patch can not be rewetted subsequent to bubble departure. The continually rising temperature spreads over the surface, thus giving rise to the burnout phenomenon.

Fiori & Bergles (1970) observed that CHF was often associated with the formation of vapour slugs/clots. They postulated that burnout occurs as a result of the evaporation of a thin liquid layer under the vapour slugs or clots, the vapour volumes preventing access of subcooled liquid to the surface [see figure 1(c)]. CHF in vertical annuli caused by the vapour–clot mechanism was studied by Rogers *et al.* (1982). CHF mechanisms in subcooled and low-quality regions were reviewed by Tong & Hewitt (1972) and Bergles (1977).

2.1.2. Annular flow

Studies of CHF mechanisms in annular flow were reviewed by Hewitt (1982). Dryout in annular flow is most commonly associated with the depletion of the liquid film by progressive entrainment, droplet deposition and evaporation. The liquid film flow rate changes axially due to the integral effect of these three factors along the channel. The limit at which the liquid film flow rate becomes zero corresponds to the onset of CHF. A critical review of CHF mechanisms for annular flow, as well as for uniformly heated surfaces, was made by Katto (1986).

2.2. CHF Mechanisms in Horizontal Flow

In horizontal channels, gravitational forces act on both the vapour phase and the liquid phase in a direction perpendicular to the fluid stream, causing asymmetric phase distribution and possibly phase separation. This maldistribution of void can have a severe effect on heat transfer in general and CHF in particular.

For flows with high mass velocities, the effect of tube orientation on CHF is negligible but for intermediate and low flows, the CHF for horizontal flow can be considerably lower. Figure 2 illustrates the possible CHF occurrences in a horizontal tube. Upstream dryout occurs in the low-quality region where bubbles coalesce and form a continuous vapour cushion along the upper portion of the tube (Becker 1971). As vaporization continues downstream, the increased stream velocity causes higher-amplitude waves to form on the liquid–vapour interface. The faster-moving

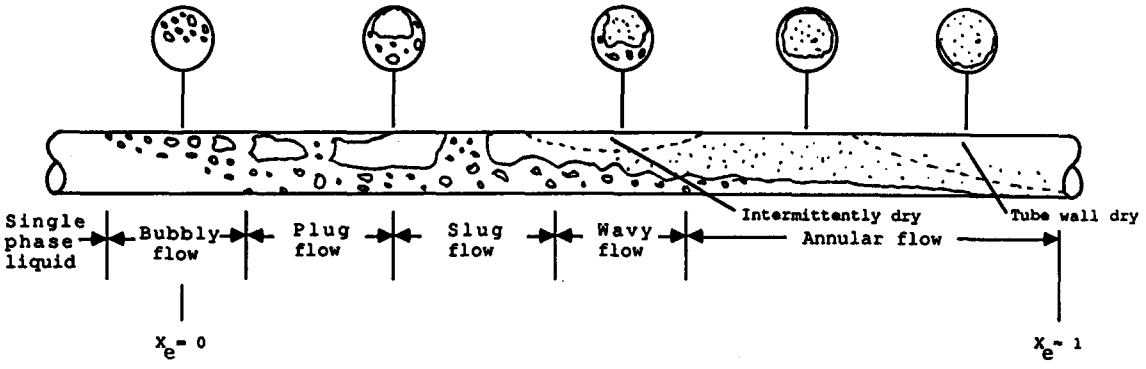

Figure 2. Flow regimes for horizontal flow (Becker 1971).

vapour stream impinges on the waves and thus causes liquid to be entrained in the vapour-core region. Some of the entrained liquid is deposited onto the upper portion of the tube and, finally, the liquid will again cover the full circumference of the tube and annular flow is established.

Studies of CHF mechanisms in different quality regions in horizontal channels have been reviewed by Fisher *et al.* (1978). They have identified the CHF mechanisms in three different quality regions.

At very low qualities, bubbles that are produced at the wall could form ribbons of vapour along the upper surface of the channel under low flow conditions. These vapour ribbons act as barriers and inhibit the replenishment of liquid lost by draining and evaporation, thus causing a premature occurrence of the CHF condition and a subsequent steep rise in the wall temperature.

At low and intermediate qualities, the flow in evaporating channels is characterized by alternating large splashing waves (surges) which carry the liquid to the upper surface of the channel. There is little or no droplet entrainment activity and, thus, no replenishment of the liquid film at the top of the channel. As a result, the liquid film at the upper surface is subjected to drainage and evaporation which will finally dryout if sufficient time is given before the next splashing wave touches the upper surface.

At high qualities, the flow pattern is probably annular. Figure 3 shows a horizontal annular flow in air and water, for typical liquid film and vapour velocities (Fisher *et al.* 1978). The annular liquid film at the top of the channel is thinner as a result of draining along the circumferential direction. At the bottom of the channel, larger-amplitude waves give rise to a significant droplet entrainment into the vapour core. Little entrainment occurs at the top of the channel because here the liquid film is much smoother. When the heat flux reaches the critical value, the liquid film at the top of the channel will become completely depleted, thus resulting in "dryout".

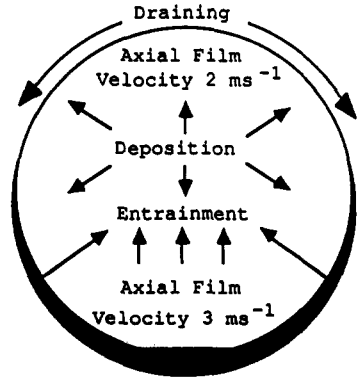

Figure 3. Horizontal annular flow in air and water (Fisher 1978).

3. FLOW STRATIFICATION CRITERIA

The correction factor (K_{hor}) is strongly dependent on the flow conditions. For values of mass flux below G_{min}, the flow is fully-stratified and hence the CHF for horizontal flow is zero or $K_{hor} = 0$. On the other hand, as mass velocities in horizontal flow are high ($G > G_{max}$), the effect of the tube orientation on CHF becomes insignificant and hence CHF_{hor} may be assumed equal to the CHF for vertical flow (CHF_{ver}). Estimates for the low and high mass flux thresholds (G_{min} and G_{max}, respectively) can be derived from Taitel & Dukler's (1986) flow-regime map.

3.1. Mass-flux Threshold for Fully-stratified Flow (G_{min})

A modified, generalized flow-regime map for horizontal flow, adapted from Taitel & Dukler (1986), is shown in figure 4. Curve D has been extended into the annular-flow regime, resulting in a subdivision of the annular regime into a homogeneous-annular regime and a stratified-annular regime (i.e. an annular-flow regime having a thinner liquid film near the top and a thicker liquid film near the bottom of the horizontal cross-section).

Taitel & Dukler (1986) studied wave stability for horizontal tube flow and derived a criterion for the boundary between stratified-wavy and intermittent or annular flow. Their criterion was in a dimensionless form dependent only on X_{LM}, the Lockhart–Martinelli parameter. Their criterion was fitted by Cheng *et al.* (1988) with reasonable accuracy:

$$F = \left(\frac{1}{0.65 + 1.11 X_{LM}^{0.6}}\right)^2, \qquad [2]$$

where F is the modified Froude number, given by

$$F = \frac{GX_a}{\sqrt{gD\rho_G(\rho_L - \rho_G)}}, \qquad [3]$$

and X_a is the actual quality. The Lockhart–Martinelli parameter is defined by

$$X_{LM} = \left(\frac{1 - X_a}{X_a}\right)^{0.9} \left(\frac{\mu_L}{\mu_G}\right)^{0.1} \left(\frac{\rho_G}{\rho_L}\right)^{0.5}. \qquad [4]$$

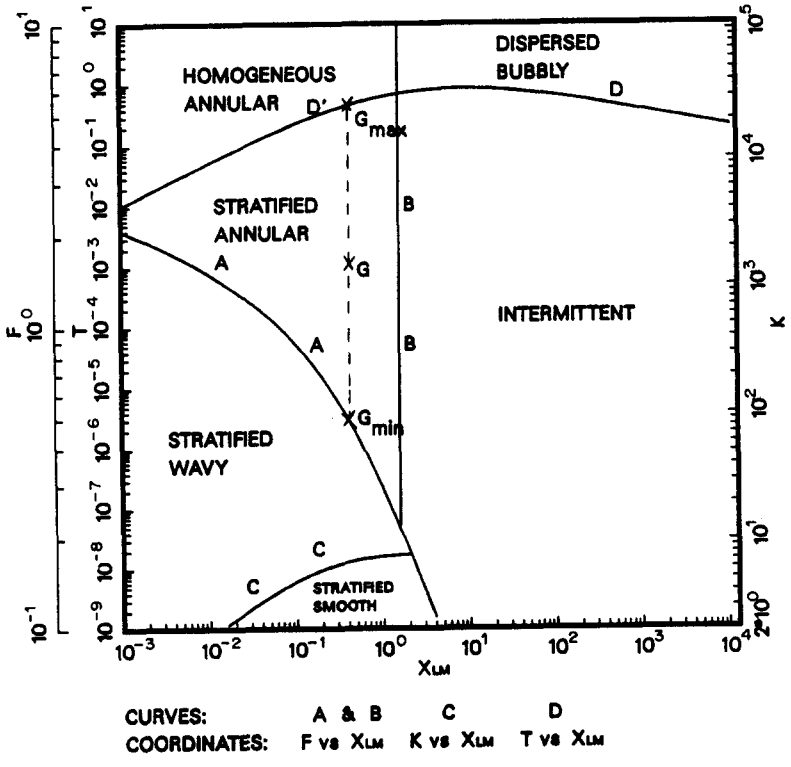

Figure 4. Modified generalized flow-regime map for horizontal flow, adapted from Taitel & Dukler (1986).

Equation [2] represents the loci of points below which fully-stratified flow occurs. It corresponds to curve A in figure 4.

Substituting [3] into [2] and rearranging, gives

$$G_{\min} = \frac{\sqrt{gD\rho_G(\rho_L - \rho_G)}}{X_a}\left(\frac{1}{0.65 + 1.11\,X_{LM}^{0.6}}\right)^2. \quad [5]$$

Equation [5] represents the minimum mass flux below which full stratification would occur for horizontal flow.

3.2. *Mass-flux Threshold for Onset of Noticeable Stratification (G_{max})*

Taitel & Dukler (1986) suggested that when the radial turbulent force is greater than the buoyancy force, bubbles will be dispersed and hence the phase distribution will not be affected by the tube orientation. Their criterion is shown as curve DD′ in figure 4 and was fitted by Cheng *et al.* (1988) to be

$$T = \exp[A + B\ln(X_{LM}) + C\ln^2(X_{LM})], \quad [6]$$

where

$$A = -0.3470, \quad B = +0.2920, \quad C = -0.0556.$$

T can be considered as the ratio of the radial turbulent force to the buoyancy force. Taitel & Dukler defined T to be

$$T = \left[\frac{\left(\frac{dP_F}{dZ}\right)_L}{g(\rho_L - \rho_G)}\right]^{0.5}. \quad [7]$$

Taitel & Dukler (1986) recommended that $f_L = 0.046\,Re_L^{-0.2}$; T can be evaluated as

$$T = \left[\frac{0.092G^{1.8}(1 - X_a)^{1.8}\mu_L^{0.2}}{gD^{1.2}\rho_L(\rho_L - \rho_G)}\right]^{0.5}. \quad [8]$$

Substituting [8] into [6] and rearranging gives the upper mass-flux threshold, i.e.

$$G_{\max} = \left[\frac{gD^{1.2}\rho_L(\rho_L - \rho_G)}{0.092(1 - X_a)^{1.8}\mu_L^{0.2}} f_2(X_{LM})^2\right]^{0.556}, \quad [9]$$

where

$$f_2(X_{LM}) = \exp[A + B\ln(X_{LM}) + C\ln^2(X_{LM})]. \quad [10]$$

The lower and higher mass-flux thresholds can be evaluated by [5] and [9], respectively. For mass velocities between the two mass-flux thresholds ($G_{\min} < G < G_{\max}$), evaluation of the CHF correction factor is required.

4. PREDICTION OF CHF IN VERTICAL TUBE FLOW

Generally, CHF in flow boiling is believed to be a function of either the local condition or the inlet condition. For uniformly heated tubes, a heat balance over the heated length L_h gives

$$X_e = \frac{4\dot{q}}{H_{LG}G}\cdot\frac{L_h}{D} - \frac{\Delta H_{in}}{H_{LG}} \quad [11]$$

and therefore a prediction method based on the local thermodynamic quality, X_e, can be transformed into a prediction method based on the inlet condition ΔH_{in}. The most common form of correlation used in practice is one of CHF against X_e. This type of correlation is often referred to as the "local condition" correlation. Two such correlations that are widely accepted are the Bowring (1972) correlation and the Biasi *et al.* (1967) correlation. (The original Bowring correlation is in the form based on the inlet condition, but can be easily rearranged into the local condition

form.) Groeneveld *et al.* (1986a) developed a table look-up method which relates CHF as a function of P, G and X_e, i.e.

$$\text{CHF} = f(P, G, X_e) \quad [12]$$

for tubes with 8 mm dia. They also provided correction factors for tube diameter, heated length etc. The method of Groeneveld *et al.* (1986a) is basically a local condition method and represents a continuation of the earlier work by Russian workers (U.S.S.R. Academy of Sciences 1977).

Both the Bowring correlation and the method of Groeneveld *et al.* (1986a) are valid for steam–water. For fluids other than steam–water, Ahmad's (1973) or Katto & Ohno's (1984) dimensionless CHF parameters can be used in conjunction with the Bowring and table look-up methods for steam–water. A generalized correlation was developed by Katto & Ohno (1984) and is valid for water as well as non-aqueous fluids. A table look-up method in dimensionless form for non-aqueous fluids was also constructed by Groeneveld *et al.* (1986b). A comparison of various CHF correlations and Groeneveld's table look-up method against tube CHF data was made by ESDU (1986) and Groeneveld *et al.* (1986a, b). Results of their comparison showed that the CHF table look-up method (Groeneveld *et al.* 1986a) is superior to the other methods. It has an r.m.s. error of 11% for 7287 water as well as non-aqueous CHF data, covering a wide range of flow conditions.

5. CHF PREDICTION FOR HORIZONTAL TUBE FLOW

5.1. Review of CHF Prediction Methods for Horizontal Tube Flow

Although there are over 500 CHF prediction methods currently available for vertical tube flow, very few methods are available to predict CHF for horizontal tube flow. *Ad hoc* correlations for the prediction of CHF in horizontal tubes have been reported by Merilo (1979), Wang & Su (1980) and Yoshida *et al.* (1987). The scarcity of horizontal CHF data is the major reason for the lack of a generalized correlation.

Merilo's (1979) correlation is one of the more acceptable correlations. He used the method of compensated distortion in deriving the horizontal CHF-modelling parameter. Merilo reported that his correlation correlates 462 freon-12 and 143 water data points (Merilo 1977; Robertson 1973) with r.m.s. errors of 9.12 and 9.07%, respectively. Merilo's correlation was tested with horizontal water CHF data collected during this study. As expected, his correlation agrees with the data from Merilo (1977) and Robertson (1973) but does not predict well other experimental values. Table 1 summarizes the results of the comparison. A graphical result of the comparison is shown in figure 5a. A large portion of the errors are found to exceed 100%.

5.2. CHF Correction Factor for Horizontal Flow

To determine the CHF for horizontal flow, Groeneveld *et al.* (1986a) suggested that the CHF for vertical flow be multiplied by a correction factor K_{hor}, i.e.

$$\text{CHF}_{hor} = K_{hor} \times \text{CHF}_{table}, \quad [13]$$

where CHF_{table} is the critical heat flux value obtained from the look-up table. This section describes several methods for deriving an expression for K_{hor}.

Table 1. Comparison of Merilo's (1979) correlation with water CHF data

Data source	No. of points	Mean[a] error (%)	r.m.s. error (%)	Pressure range (MPa)
Robertson (1973)	52	3.65	8.90	3.4–6.9
Leontiev *et al.* (1981)	23	−7.68	30.19	6.9–13.7
Becker (1971)	94	76.07	124.38	1.0–3.0
Merilo (1977)	34	−2.48	7.99	6.9–9.7
Kohler & Hein (1986)	69	55.80	81.36	10, 15, 20
Wang & Su (1980)	19	−68.16	69.33	4.9
All data	291	33.1	82.2	

[a]Mean of $\dfrac{\text{CHF}_{pred} - \text{CHF}_{expt}}{\text{CHF}_{expt}}$.

5.3. Mass-flux Threshold Methods

Groeneveld (1982) suggested that when flow is fully stratified, the CHF is zero and hence $K_{hor} = 0$. On the other hand, as mass velocities in horizontal flow are high, the effects of tube orientation on the CHF become insignificant and hence CHF_{hor} may be assumed equal to CHF for vertical flow (CHF_{ver}). The lower and higher mass-flux thresholds (G_{min} and G_{max}, respectively) can be calculated for any set of given flow conditions, as outlined in sections 3.1 and 3.2. For flow conditions between the two mass-flux thresholds, K_{hor}varies and depends on the flow parameters G, X_e, P and D. A simplified expression for the K_{hor} factor was suggested by Groeneveld *et al.* (1986a) which assumes a linear relationship between the K_{hor} factor and the mass flux. The expression is shown as follows:

$$K_{hor} = \left(\frac{G - G_{min}}{G_{max} - G_{min}}\right), \qquad [14]$$

where

$$K_{hor} = 0 \quad \text{for} \quad G < G_{min},$$

$$K_{hor} = 1 \quad \text{for} \quad G > G_{max}.$$

This approach has the correct asymptotic trends at the two mass-flux thresholds, i.e. when the flow is fully stratified ($G \leqslant G_{min}$), the CHF will be zero and when the mass velocity is high ($G \geqslant G_{max}$), the CHF for horizontal flow will be equal to that for vertical flow. The mass-flux threshold method is not valid for zero gravity. However, it must be noted that for zero gravity, tube orientation (vertical or horizontal) becomes meaningless and thus no CHF correction factor is necessary.

A comparison with CHF data showed that the linear mass-flux interpolation, [14], is not adequate in predicting the CHF correction factor. A simple modification to include a non-linear mass relationship helped to improve the CHF_{hor} prediction. A form of

$$K_{hor} = \left(\frac{G - G_{min}}{G_{max} - G_{min}}\right)^n \qquad [15]$$

was suggested because it has the correct parametric trends. Equation [15] was used to correlate 291 horizontal water CHF data points. With least-squares curve fitting, an optimum form of [15] was found to be

$$K_{hor} = \left(\frac{G - G_{min}}{G_{max} - G_{min}}\right)^{0.62}. \qquad [16]$$

The results of the comparison with horizontal water CHF data are summarized in table 2. A significant improvement was noted with the use of [16]. The prediction error based on [16] was plotted against the critical equilibrium quality and is shown in figure 5b. The errors are calculated based on a constant inlet condition.

5.4. Force-balance and Transit-time Approach

Extrapolation of Taitel & Dukler's (1986) transition criterion between the intermittent flow and the dispersed bubbly flow (curve D, figure 4) into the annular flow regime is questionable. A more mechanistic approach for the estimation of the CHF correction factor was developed based on a force-balance and transit-time ratio analysis.

5.4.1. Force-balance approach

For annular flow, the buoyancy force per unit length of the gas region is

$$F_B = g(\rho_L - \rho_G)A_G \qquad [17]$$

and the radial turbulent force per unit length is

$$F_T = \tfrac{1}{2}\rho_L v'^2 p_i, \qquad [18]$$

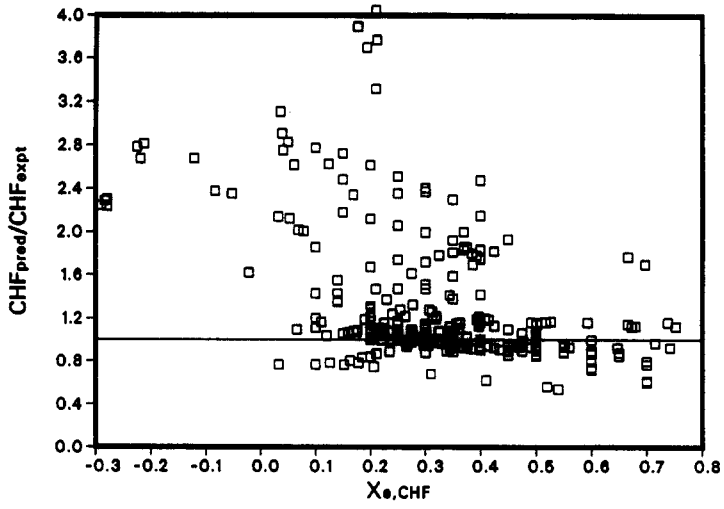

Figure 5a. Comparison of predicted and experimental CHF for water using Merilo's method.

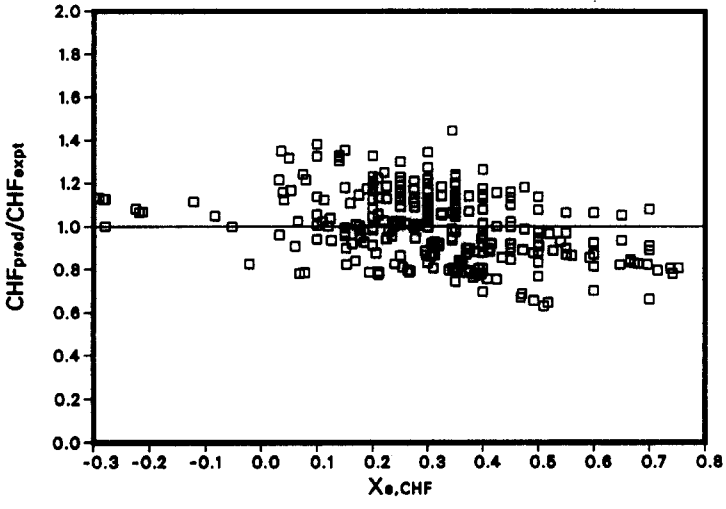

Figure 5b. Comparison of predicted and experimental CHF for water using [16].

where v' is the radial velocity fluctuation and p_i is the interface perimeter (see figure 6). The turbulent to buoyancy force ratio can be used as a measure of the degree of stratification. Defining a parameter T_1 as

$$T_1 = \frac{F_T}{F_B} = \frac{\frac{1}{2}\rho_L v'^2 p_i}{g(\rho_L - \rho_G)A_G}. \quad [19]$$

For annular flow, p_i is evaluated as

$$p_i = \pi D_i \quad [20]$$

and

$$\frac{D_i^2}{D^2} = \frac{A_G}{A} = \epsilon, \quad [21]$$

where ϵ is the cross-sectional average void fraction. Therefore,

$$D_i = D\epsilon^{0.5}. \quad [22]$$

Table 2. Comparison of horizontal water CHF data with various correlations for constant inlet conditions

Equation	Mean[a] error	r.m.s. error	Standard deviation	Fraction of data[b] within a prediction accuracy of: 10%	20%	50%
[14]	−0.214	0.296	0.201	0.2887	0.4914	0.8866
[16]	−0.021	0.160	0.159	0.3677	0.7973	1.0000
[36]	−0.031	0.156	0.153	0.4296	0.7938	1.0000
Merilo (1979)	0.331	0.822	0.632	0.3368	0.5395	0.6838
Wang & Su (1980)	Prediction is impossible for many CHF data due to the wrong parametric trend of the correlation					

[a]Mean of $\dfrac{CHF_{pred} - CHF_{expt}}{CHF_{expt}}$.

[b]No. of data points = 291.

Substituting [20] and [22] into [19] gives

$$T_1 = \frac{\frac{1}{2}\rho_L v'^2 \pi D \epsilon^{0.5}}{g(\rho_L - \rho_G)A_G}. \quad [23]$$

The portion of the cross-section occupied by vapour (A_G) can be expressed in terms of the void fraction. Thus, rearranging [23] yields

$$T_1 = \frac{2\rho_L v'^2}{gD(\rho_L - \rho_G)\epsilon^{0.5}}. \quad [24]$$

Taitel & Dukler (1986) argued that the r.m.s. value of v' is approximately equal to the friction velocity. Thus,

$$(\bar{v}'^2)^{1/2} = u^* = u_L\left(\frac{f_L}{2}\right)^{1/2}. \quad [25]$$

Substituting [25] into [24] yields

$$T_1 = \frac{2\rho_L u_L^2\left(\frac{f_L}{2}\right)}{gD(\rho_L - \rho_G)\epsilon^{0.5}}. \quad [26]$$

Taitel & Dukler recommended $f_L = 0.046\,Re_L^{-0.2}$ for turbulent flow. Substitution into [26] gives

$$T_1 = 0.046\,Re_L^{-0.2}\left(\frac{1 - X_a}{1 - \epsilon}\right)^2 \frac{G^2}{gD\rho_L(\rho_L - \rho_G)\epsilon^{0.5}}. \quad [27]$$

The parameter T_1 can be used as a measure of the dominance of the turbulent force over the buoyancy force. It has the correct parametric trends with G, X_a, D and P.

Similar force-balance parameters in bubbly- and droplet-flow regimes were also derived (Wong 1988). Table 3 summarizes all the parameters derived.

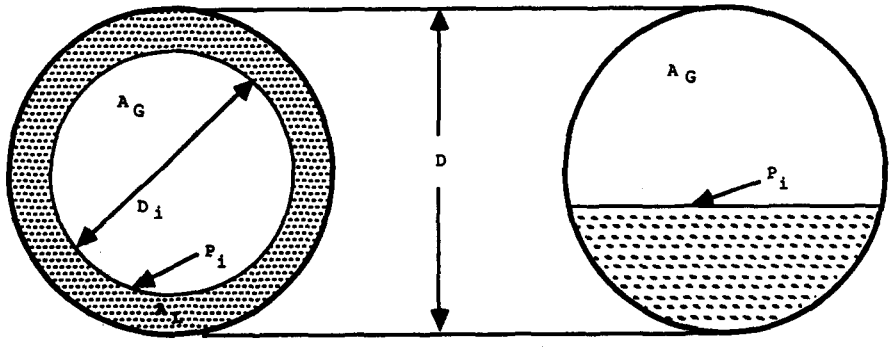

Figure 6. Interface perimeters for annular flow and equilibrium stratified flow.

Table 3. Summary of dimensionless parameters (Wong 1988)

Notation	Equation form
T_1	$C_1 Re_L^{-0.2}\left(\frac{1-X_a}{1-\epsilon}\right)^2 \frac{G^2}{gD\rho_L(\rho_L-\rho_G)\epsilon^{0.5}}$
T_2	$C_2\left(\frac{\rho_G}{\rho_L}\right)\frac{G^4}{g\sigma\rho_L^2(\rho_L-\rho_G)}\left[\frac{\frac{\rho_L}{\rho_G}(1-\epsilon)X_a-\epsilon(1-X_a)}{\epsilon(1-\epsilon)}\right]^4$
T_3	$C_3 Re_L^{-0.2}\rho_G^2\frac{u_L^2(u_G-u_L)^2}{g(\rho_L-\rho_G)}$
T_4	$C_4\left(\frac{\rho_G}{\rho_L}\right)\frac{G^4}{g\sigma\rho_L^2(\rho_L-\rho_G)}\left[\frac{\frac{\rho_L}{\rho_G}(1-\epsilon)X_a-\epsilon(1-X_a)}{\epsilon(1-\epsilon)}\right]^4$
T_5	$C_5\frac{G}{\sqrt{gD\rho_G(\rho_L-\rho_G)}}\left(\frac{X_a}{\epsilon}\right)\left(\frac{D}{L_h}\right)$
T_6	$C_6\frac{G}{\sqrt{gD\rho_L(\rho_L-\rho_G)}}\left(\frac{1-X_a}{1-\epsilon}\right)\left(\frac{D}{L_h}\right)$

T_1—turbulent/buoyant force (annular).
T_2—drag/buoyant force (bubbly).
T_3—turbulent/buoyant force (bubbly).
T_4—drag/buoyant force (droplet).
T_5—transit-time ratio (bubbly).
T_6—transit-time ratio (droplet).

5.4.2. Transit-time approach

The transit time taken for a droplet or bubble to travel across the channel is compared to the transit time to travel along the channel. This transit-time ratio serves as a measure of void migration and hence a measure of the void accumulation near the top of the channel. Some simplified approaches were utilized in the development of the transit-time ratio for various types of flow regimes such as droplet flow and bubbly flow.

For bubbly flow, the bubbles have an average velocity proportional to the exit velocity, i.e.

$$u_G = \text{const}\cdot\frac{GX_a}{\rho_G\epsilon}, \qquad [28]$$

where X_a and ϵ are the actual quality and void fraction at the exit, respectively. The constant will be absorbed by another constant in the correlation process later. Hence it can be assumed to be 1.0 here. Therefore, the time taken for the bubble to travel to the exit is given by

$$t_x = \frac{L_h}{u_G} \qquad [29]$$

or

$$t_x = \frac{\rho_G\epsilon}{GX_a}L_h. \qquad [30]$$

By neglecting the drag force in the vertical direction, the force balance in the vertical direction is

$$\frac{\pi d^3}{6}\rho_G\frac{du_y}{dt} = \frac{\pi d^3}{6}(\rho_L-\rho_G)g, \qquad [31]$$

where u_y = upward bubble velocity.

Assuming average bubbles start to depart at the middle of the tube, the bubble rise time can be found by integrating the velocity with respect to time over the distance $D/2$, thus

$$t_y = \left[\frac{D\rho_G}{g(\rho_L-\rho_G)}\right]^{1/2}. \qquad [32]$$

Therefore, the transit-time ratio is defined as

$$T_5 = \frac{t_y}{t_x} = \frac{G}{\sqrt{gD\rho_G(\rho_L - \rho_G)}} \frac{X_a}{\epsilon} \frac{D}{L_h}. \quad [33]$$

Similarly, the transit-time ratio for droplet flow was derived (Wong 1988) as

$$T_6 = \frac{t_y}{t_x} = \frac{G}{\sqrt{gD\rho_L(\rho_L - \rho_G)}} \left(\frac{1 - X_a}{1 - \epsilon}\right) \frac{D}{L_h}. \quad [34]$$

5.4.3. Correlation for K_{hor}

Attempts were made to relate the CHF ratio (CHF_{hor}/CHF_{ver}) to the parameters developed. The following simple exponential expression, which has the correct parametric trends, was found to be suitable for correlating the CHF correction factor:

$$K_{hor} = 1 - \exp\left[-\left(\frac{T_i}{A}\right)^B\right], \quad [35]$$

where T_i represents T_1 to T_6 shown in table 3. All six parameters in table 3 were tested in the derivation of the CHF correction factor (Wong 1988). Using the least-squares fit, optimum values for A and B were obtained for each case which gives the respective minimum r.m.s. errors. Table 4 summarizes the error distributions for each parameter tested based on constant inlet conditions. The best correlation appears to be with the use of parameter T_1 with B = 0.5 and A = 3.0:

$$K_{hor} = 1 - \exp\left[-\left(\frac{T_1}{3}\right)^{0.5}\right]. \quad [36]$$

The void fraction is required in the evaluation of parameter T_1. The CISE void correlation (Premoli *et al.* 1970) was chosen for this case because it is the most accurate generally applicable correlation (Whalley 1987). Equation [36] correlates 291 water data and 203 freon-12 data with r.m.s. errors of 15.6 and 15.4%, respectively.

Table 4. Comparison of horizontal water CHF data with [35] for various parameters and constants (constant inlet conditions approach)

Equation	Mean[a] error	r.m.s. error	Standard deviation	Fraction of data[b] within a prediction accuracy of: 10%	20%	50%
$1-\exp\left[-\left(\frac{T_1}{2.53}\right)^{0.5}\right]$	0.006	0.161	0.161	0.4502	0.7526	1.0000
$1-\exp\left[-\left(\frac{T_1}{2.76}\right)^{0.5}\right]$	−0.012	0.157	0.156	0.4124	0.7663	1.0000
$1-\exp\left[-\left(\frac{T_1}{3.0}\right)^{0.5}\right]$	−0.031	0.156	0.153	0.4296	0.7938	1.0000
$1-\exp\left[-\left(\frac{T_1}{3.22}\right)^{0.5}\right]$	−0.044	0.157	0.151	0.4296	0.8041	1.0000
$1-\exp\left[-\left(\frac{T_3}{20}\right)^{0.5}\right]$	−0.011	0.445	0.442	0.4192	0.4811	0.7113
$1-\exp\left[-\left(\frac{T_5}{0.06}\right)^{0.9}\right]$	−0.093	0.284	0.249	0.3849	0.6151	0.8900
$1-\exp\left[-\left(\frac{T_5}{0.065}\right)^{0.8}\right]$	−0.077	0.259	0.230	0.4330	0.6392	0.9107

[a]Mean of $\frac{CHF_{pred} - CHF_{expt}}{CHF_{expt}}$.

[b]No. of data points = 291.

Table 5. Comparison of horizontal freon-12 CHF data with various correlations for the constant inlet conditions approach

Equation	Mean[a] error	r.m.s. error	Standard deviation	Fraction of data[b] within a prediction accuracy of: 10%	20%	50%
[14]	+0.102	0.148	0.107	0.4828	0.8473	1.0000
[16]	+0.097	0.175	0.111	0.4729	0.8473	1.0000
[36]	+0.045	0.154	0.147	0.4532	0.8177	1.0000
Merilo (1979)	−0.052	0.115	0.104	0.5616	0.9310	1.0000
Wang & Su (1980)	Prediction is impossible for many CHF data due to the wrong parametric trend of the correlation					

[a]Mean of $\frac{CHF_{pred} - CHF_{expt}}{CHF_{expt}}$.

[b]No. of data points = 203.

6. COMPARISON OF RESULTS

In the analyses presented above, actual vapour quality is required—while in practice the thermodynamic quality is the quantity usually known. For qualities >20%, the thermodynamic quality can be assumed equal to that of the actual quality. For subcooled and low-quality flow boiling, the actual quality can be estimated from Saha & Zuber's (1974) equation.

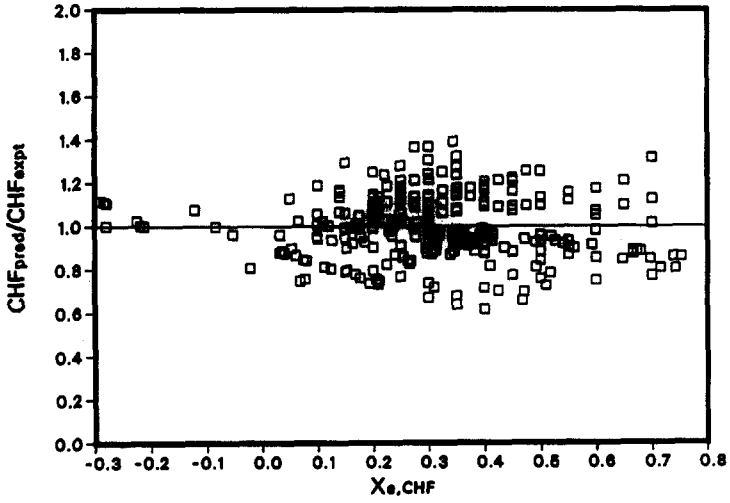

Figure 7a. Comparison of predicted and experimental CHF for water using [36].

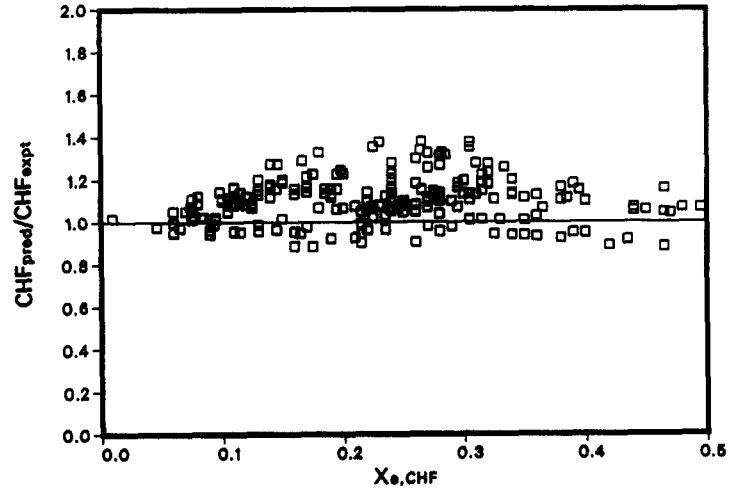

Figure 7b. Comparison of predicted and experimental CHF for freon-12 using [36].

A comparison between the different methods developed and Merilo's correlation for water is summarized in table 2. Equation [36] has a better overall prediction accuracy. The comparison for freon-12 is shown in table 5. Similar trends of errors are observed.

Prediction errors for both water and freon-12 data are also presented in figures 7a and 7b. The applicability of [36] to non-aqueous fluids is partially confirmed by the freon-12 data comparison even though the correlation constants were optimized based on water data only. This is because the dimensionless parameters were derived analytically, based on fluid properties such as densities, viscosity and surface tension, regardless of the type of fluid involved.

Comparison was made for constant inlet conditions because the inlet conditions of the experimental data were given. With the given inlet parameters (hence constant inlet conditions) and heated length, an energy-balance equation can be drawn as shown in figure 8. An initial CHF_{hor} is assumed, the exit quality $X_{e,CHF}$ can be located from the energy-balance line. This $X_{e,CHF}$ is then used as the local parameter for the determination of CHF_{ver} and K_{hor}. The first estimate of CHF_{hor} can thus be obtained from [1]. If this calculated CHF_{hor} is different from the CHF_{hor} initially assumed, the average value will be used for the new estimation of $X_{e,CHF}$ and hence new CHF_{hor}. The iteration process continues until converging to a desired tolerance.

Under certain flow conditions (high pressure and high mass flux), [36] could underpredict the CHF_{hor} considerably. It is due to the slow approach of the exponential function towards the value of 1.0 even for mass flux values sufficiently high to suppress the gravitational effect. Figure 9 shows the variation of CHF correction factor with mass flux as predicted by [14] and [36]. For mass flux greater than G_A, [14] predicts higher values of CHF correction factor and thus converges towards the value of 1.0 sooner. Taking the maximum value of the two predictions will avoid the problem of serious under-predictions. CHF_{hor} values, predicted from this maximum value approach were compared to 291 water data points and resulted in a lower r.m.s. error (14.9%). A similar comparison was made for 203 freon-12 data points and the r.m.s. error was found to be 16%.

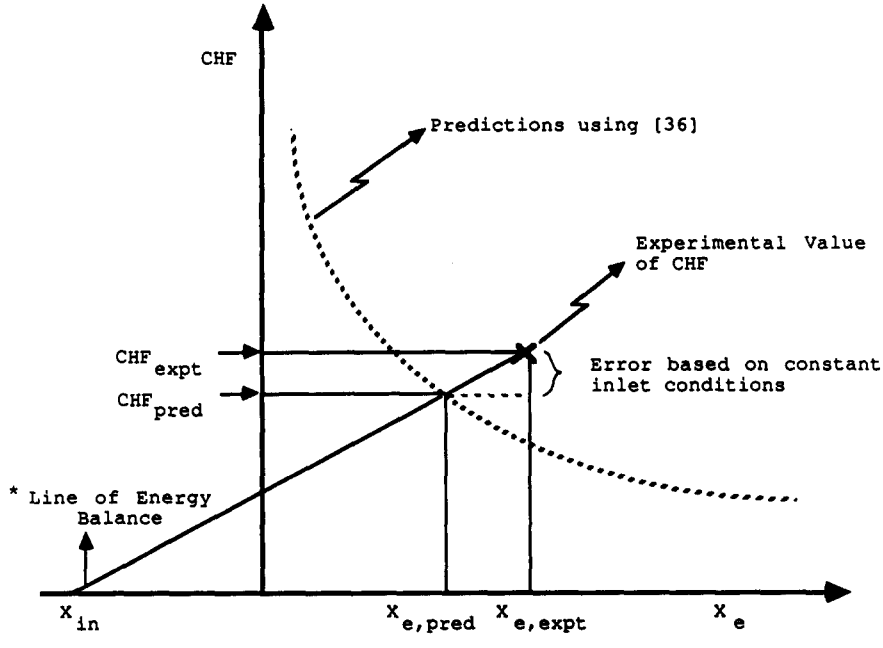

Figure 8. Error based on constant inlet conditions. *Energy balance is calculated from the following equation:

$$X_e = \frac{4\dot{q}}{H_{LG}G} \times \frac{L_h}{D} - X_{in}.$$

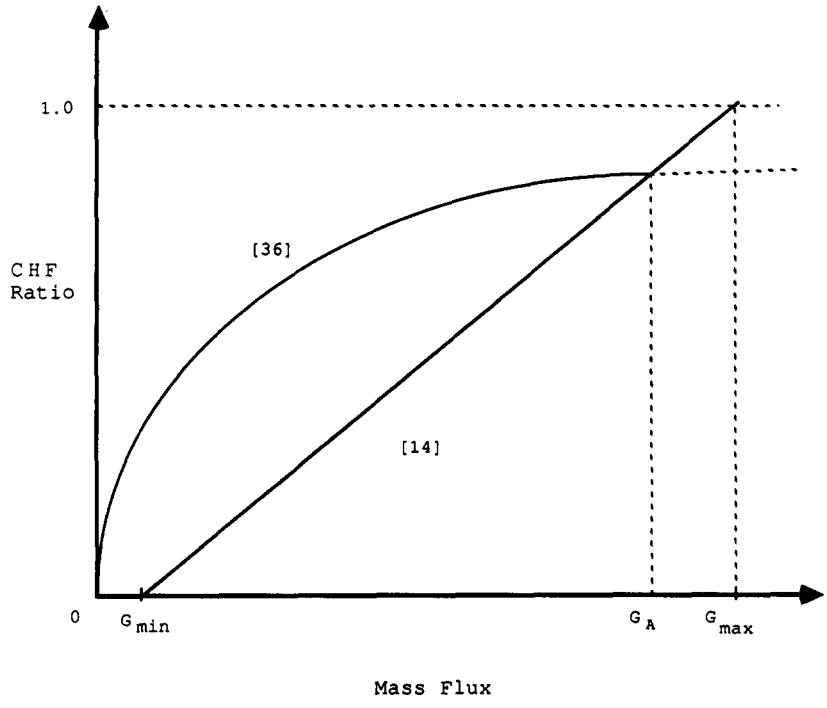

Figure 9. CHF ratio prediction as a function of mass flux.

7. CONCLUSIONS AND FINAL REMARKS

A prediction method for CHF in horizontal flow was developed in this study. This prediction method has been found to agree with experimental CHF data obtained for uniformly heated tubes. It is valid for water as well as freon-12. The parameters T_1 to T_6 were used to correlate the CHF data for specific flow regimes (Wong 1988). It was found that T_1 can be used to correlate the CHF ratio accurately over the widest range of flow parameters. Equation [36] appears to be reasonably accurate and applicable over a wide range of flow parameters and for different fluids. The r.m.s. errors for [36] for 291 water data points and 203 freon-12 data points are 15.6 and 15.4%, respectively. Although [14] is inadequate for predicting water CHF, it appears to be quite accurate for predicting freon-12 CHF (with 14.8% r.m.s. error). Merilo's (1979) correlation appears to be the most accurate in predicting the freon-12 data because the same data base was among those used in the derivation of his correlation.

Better predictions could result if the data were classified into different flow regimes [e.g. using Taitel & Dukler's (1986) flow-regime map] and if attempts were made to correlate the data with different T_i for different flow regimes. An experimental investigation on void migration in horizontal tube is underway at the Chalk River Nuclear Laboratories (CRNL). A better transit-time ratio model may be developed later based on this work.

Acknowledgements—The authors would like to thank Atomic Energy of Canada Limited (AECL), the National Science and Engineering Research Council (NSERC) and the Heat Transfer and Fluid Flow Service (HTFS) for their financial support.

REFERENCES

AHMAD, S. Y. 1973 Fluid to fluid modelling of critical heat flux: a compensated distortion model. *Int. J. Heat Mass Transfer* **16**, 641–662.

BECKER, K. M. 1971 Measurement of burnout conditions for flow of boiling water in horizontal round tubes. Report No. AERL-1262, Atomenergia-Aktieb, Sweden.

BERGLES, A. E. 1977 Burnout in boiling heat transfer. Part II: subcooled and low-quality forced-convection systems. *Nucl. Saf.* **18**, 154–167.

BIASI, L., CLERICI, G. C., TARRIBBA, S., SALA, R. & TOZZI, A. 1967 Studies on burnout: Part 3. *Energia nucl., Milano* **14**, 530–536.

BOWRING, R. W. 1972 A simple but accurate round tube uniform heat flux, dryout correlation over the pressure range 0.17–17 MN/m^2 (100–2500 psia). Report AEEW-R789, UKAEA, Winfrith, Dorset.

CHENG, S. C., WONG, Y. L. & GROENEVELD, D. C. 1988 CHF prediction for horizontal flow. In *Proc. Int. Symp. on Phase Change Heat Transfer*, Chongqing, China, pp. 211–215.

ESDU 1986 Boiling inside tubes: critical heat flux for upward flow in uniformly heated vertical tubes. Engineering Sciences Data Unit Item No. 860323, 251–259 Regent St, London.

FIORI, M. P. & BERGLES, A. E. 1970 Model of critical heat flux in subcooled flow boiling. In *Proc. 4th Int. Heat Transfer Conf.*, Versailles, Paper B6.3.

FISHER, S. A., HARRISON, G. S. & PEARCE, D. C. 1978 Premature dryout in conventional and nuclear power station evaporators. In *Proc. 6th Int. Heat Transfer Conf.*, Toronto, Vol. 2, pp. 49–54.

GROENEVELD, D. C. 1982 A general CHF prediction method for water, suitable for reactor accident analysis. CENG Report DRE/STT/SETRE/82-2-E/DG.

GROENEVELD, D. C., CHENG, S. C. & DOAN, T. 1986a 1986 AECL-UO critical heat flux lookup table. *Heat Transfer Engng* **7**, 46–62.

GROENEVELD, D. C., KIAMEH, B. P. & CHENG, S. C. 1986b Prediction of critical heat flux (CHF) for non-aqueous fluids in forced convective boiling. In *Proc. 8th Int. Heat Transfer Conf.*, San Francisco, Calif., Paper FB-15, pp. 2209–2214.

HEWITT, G. F. 1982 Burnout. In *Handbook of Multiphase Systems* (Edited by HETSRONI, G.) pp. 6.66–6.141. McGraw-Hill, New York.

KATTO, Y. 1986 Critical heat flux in boiling. Keynote paper presented at the *8th Int. Heat Transfer Conf.*, San Francisco, Calif., Vol. 1, pp. 171–180.

KATTO, Y. & OHNO, H. 1984 An improved version of the generalized correlation of critical heat flux for the forced convective boiling in uniformly heated vertical tubes. *Int. J. Heat Mass Transfer* **27**, 1641–1648.

KIRBY, G. J., STAINFORTH, R. & KINNEIR, L. H. 1967 A visual study of forced convection boiling. 2. Flow patterns and burnout for a round test section. Report AEEW-506, UKAEA, Winfrith, Dorset.

KOHLER, W. & HEIN, D. 1986 Influence of the wetting state of a heated surface on heat transfer and pressure loss in an evaporator tube. International Agreement Report NUREG/IA-0003, pp. 63–79.

KUTATELADZE, S. S. & LEONTIEV, A. I. 1966 Some applications of the asymptotic theory of the turbulent boundary layers. In *Proc. 3rd Int. Heat Transfer Conf.*, Chicago, Ill., Vol. 3, pp. 1–6.

LEONTIEV, A. I., MOSTINSKY, I. L., POLONSKY, V. S., STYRIKOVICH, M. A. & CHERNIKA, I. M. 1981 Experimental investigation of the critical heat flux in horizontal channels with circumferentially variable heating. *Int. J. Heat Mass Transfer* **24**, 821–828.

MERILO, M. 1977 Critical heat flux experiments in a vertical and horizontal tube with both freon-12 and water as coolant. *Nucl. Engng Des.* **44**, 1–16.

MERILO, M. 1979 Fluid-to-fluid modeling and correlation of flow boiling crisis in horizontal tubes. *Int. J. Multiphase Flow* **5**, 313–325.

MERILO, M. & AHMAD, S. Y. 1979 Experimental study of CHF in vertical and horizontal tubes cooled by freon-12. *Int. J. Multiphase Flow* **5**, 463–478.

PREMOLI, A., FRANCESCO, D. & PRINA, A. 1970 An empirical correlation for evaluating two-phase mixture density under adiabatic conditions. Presented at the *Eur. Two-phase Flow Gp Mtg*, Milan [cited in Whalley (1987)].

ROBERTSON, J. M. 1973 Dryout in horizontal hairpin waste-heat boiler tubes. *AIChE Symp. Ser.* **69**, 55–72.

ROGERS, J. T., SALCUDEAN, M. & TAHIR, A. 1982 Flow boiling critical heat fluxes in a vertical annulus at low pressure and velocities. In *Proc. 7th Int. Heat Transfer Conf.*, Munich, Vol. 4, pp. 339–344.

SAHA, P. & ZUBER, N. 1974 Point of net vapor generation and vapor void fraction in subcooled boiling. In *Proc. 5th Int. Heat Transfer Conf.*, Tokyo, Vol. 4, pp. 175–179.

TAITEL, Y. & DUKLER, A. E. 1986 Flow pattern transition in gas–liquid systems: measurement and modelling. In *Multiphase Science and Technology*, Vol. 2 (Edited by HEWITT, G. F., DELHAYE, J. M. & ZUBER, N.), pp. 1–94. Hemisphere, Washington, D.C.

TONG, L. S. 1972 Boiling crisis and critical heat flux. USAEC Critical Review Series, Report TID-25887.

TONG, L. S. & HEWITT, G. F. 1972 Overall viewpoint of film boiling CHF mechanisms. ASME Paper 72-HT-54.

U.S.S.R. ACADEMY OF SCIENCES 1977 Tabular data for calculating burnout when boiling water in uniformly heated round tubes. *Therm. Engng* **Sept.,** 77–79; *Teploenergitika* **23,** 90–92 (1976).

WANG, J. M. & SU, C. H. 1980 Dryout quality and post-dryout heat transfer coefficient of steam–water mixture flowing in a horizontal pipe. Presented at the *Int. Semin. Nuclear Reactor Safety Heat Transfer*, Dubrovnik.

WHALLEY, P. B. 1987 *Boiling, Condensation and Gas–Liquid Flow; Oxford Engineering Science Series*. Oxford Univ. Press, New York.

WONG, Y. L. 1988 Generalized CHF prediction for horizontal tubes with uniform heat flux. M.A.Sc. Thesis, Univ. of Ottawa, Ontario.

YOSHIDA, S., MORI, H. & OHNO, M. 1987 Critical heat flux for boiling freon at high subcritical pressure in horizontal tubes. Presented at the *Joint ASME–JSME Thermal Engineering Conf.*, Honolulu, Hawaii.